Supporting Information for

Non-invasive and Highly Selective Monitoring of Intracellular Glucose *via* Two-steps Recognition-based Nanokit

Jianru Tang[†], Dandan Ma[†], Stevan Pecic[§], Caixia Huang[†], Jing Zheng[†,*], Jishan Li[†], Ronghua Yang[†,‡,*]

[†]State Key Laboratory of Chemo/Biosensing and Chemometrics, College of Chemistry and Chemical Engineering, Hunan University, Changsha, 410082, China; [‡]School of Chemistry and Biological Engineering, Changsha University of Science and Technology, Changsha, 410082, China; [§]University Medical Center, Columbia University, New York, 10032, USA

*To whom correspondence should be addressed:

E-mail: zhengjing2013@hnu.edu.cn; Yangrh@pku.edu.cn

Fax: +86-731-8882 2523

EXPERIMENTAL SECTION

Instruments. Transmission electron microscopy images obtained on JEM-100CXII microscope (JEOL, Ltd., Japan). UV-Vis absorption spectra were recorded on a Hitachi U-4100 UV/Vis spectrophotometer (Kyoto, Japan). Fluorescence images of cells were obtained using an Olympus FV1000-MPE multiphoton laser scanning confocal microscope (Japan).The pH was measured with a model 868 pH meter (Orion).

Table S1. Oligonucleotides Used in This Work*

Entry	Sequence (5′-3′)
Capture sequence	TGT CGT CCC GAG AGT TTT TTT-SH
Aptamer sequence	TAMRA-CTC TCG GGA CGA CAG CCG AGT TGA TTC AAC AGC CGA GTC GTC CC

Table S2. Determination of Glucose in Cell Lysate

Sample	Added (μM)	Measured (μM)	Recovery (%)
1	0	0.27±0.3	---
2	50	51±1.4	101
3	100	98±2.6	98

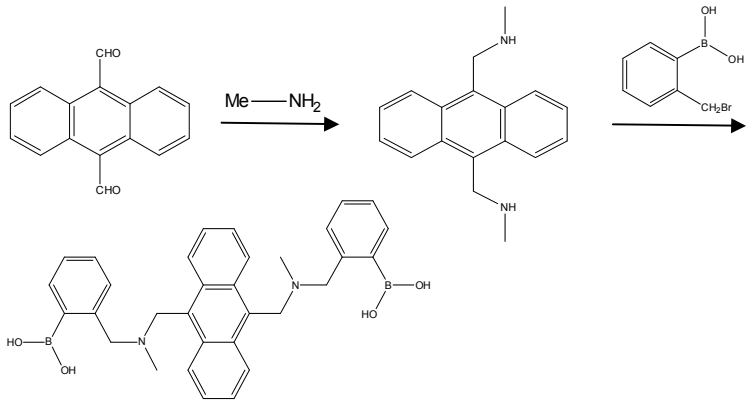

Figure S1. The synthetic route of the Shinkai's receptor.

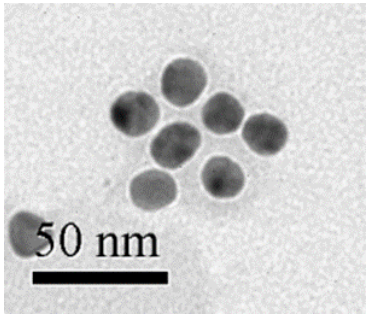

Figure S2. Representative TEM image of AuNPs.

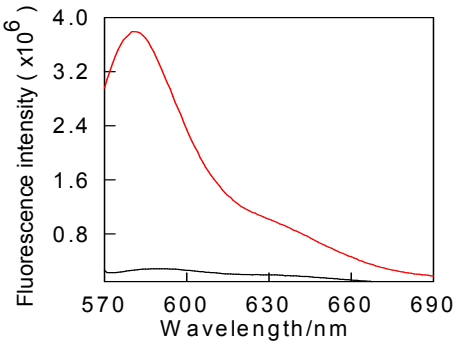

Figure S3. Fluorescence spectrum of TAMRA-labeled aptamer before (red curve) and after (black curve) conjugation to the surface of AuNPs.

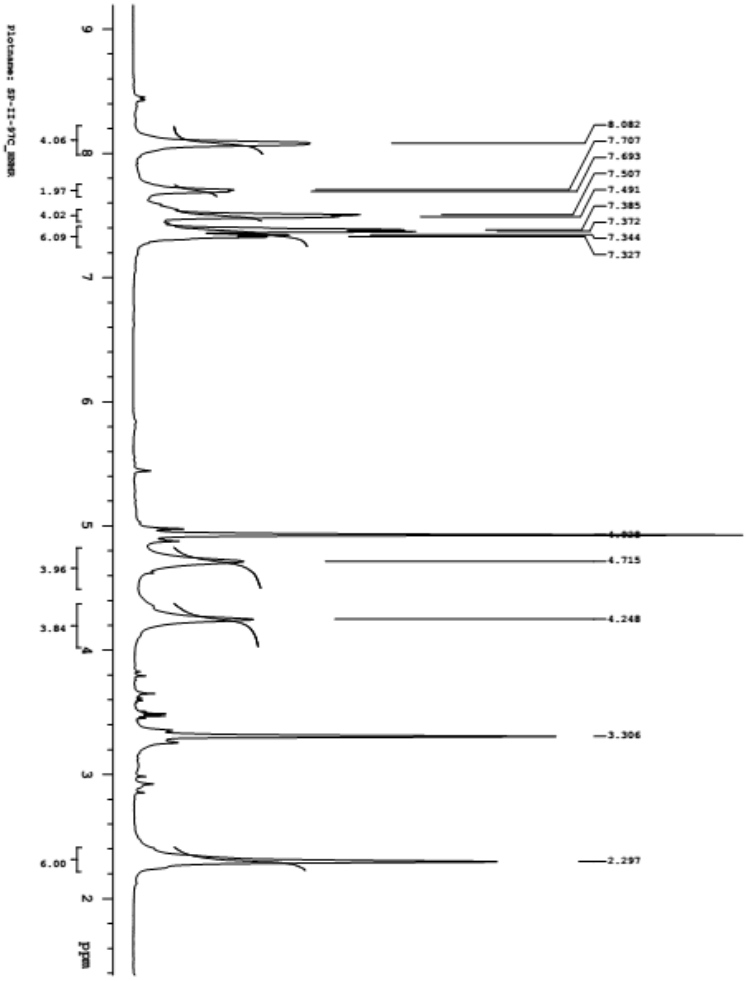

Figure S4. 1H NMR of the Shinkai's receptor.

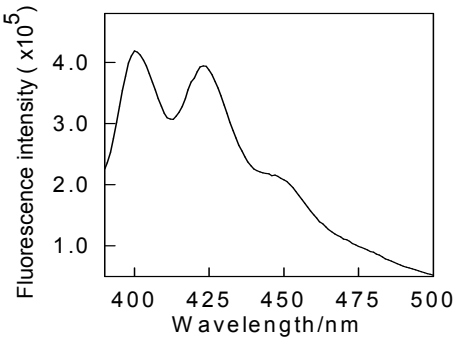

Figure S5. Fluorescence spectrum of the Shinkai's receptor. The excitation wavelength was 370 nm.

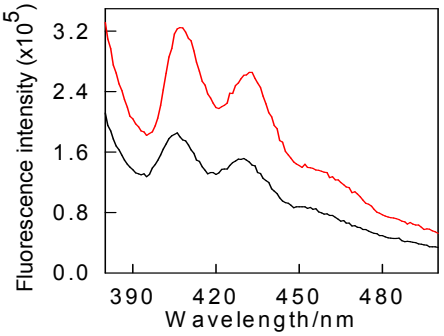

Figure S6. Fluorescence spectrum of the Shinkai's receptor-encapsulated liposomes before (black curve) and after (red curve) Triton X-100 treated. The excitation wavelength was 370 nm.

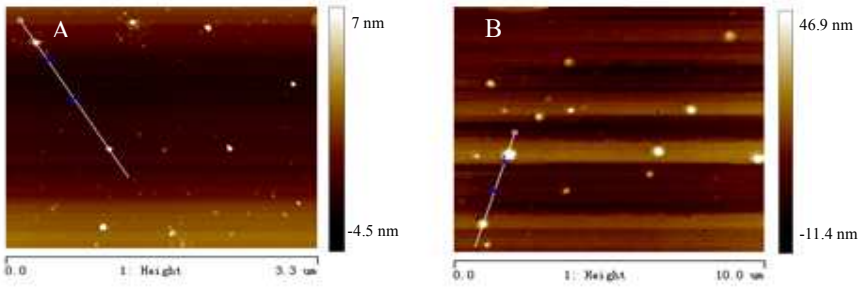

Figure S7. Representative AFM images of AuNPs (A) the synthetic Shinkai's receptor-encapsulated liposome (B).

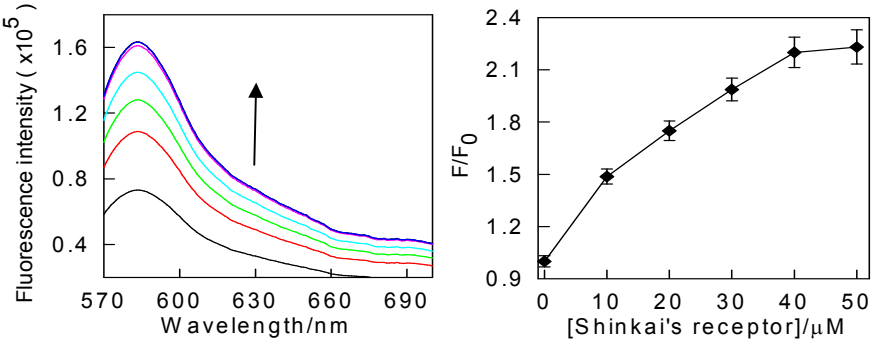

Figure S8. The fluorescence recovery of AuNP@ODs upon 10 mM glucose addition with aid of different concentrations of the Shinkai's receptor.

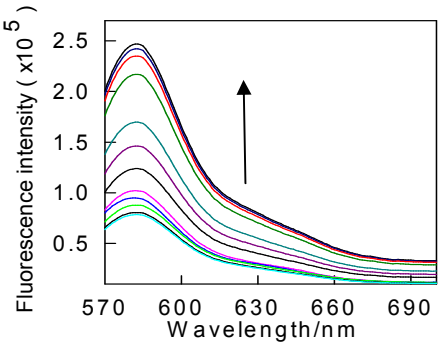

Figure S9. Representative fluorescence spectrum of AuNP@ODs (10 nM) as functions of different concentrations of glucose with aid of the Shinkai's receptor (50 μM). The arrows indicate the concentration from 0 to 2 mM (0, 0.1, 0.5, 1, 10, 100, 250, 500, 1000, 1500, 1750, 2000 μM).

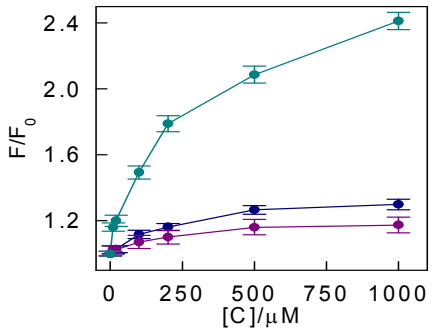

Figure S10. The fluorescence recovery of AuNP@ODs (10 nM) upon different concentration of glucose, galactose and fructose addition with aid of Shinkai's receptor (50 μM).

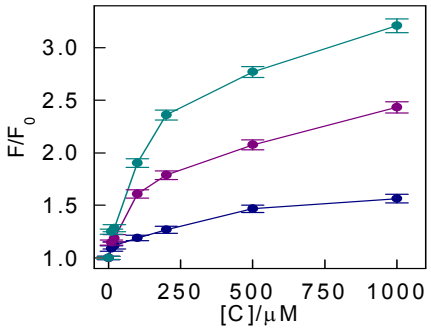

Figure S11. The fluorescence recovery of the Shinkai's receptor (50 μM) upon different concentration of glucose, fructose and galactose.

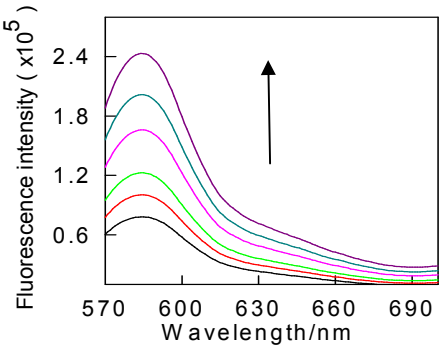

Figure S12. Fluorescence spectra of nanokit upon addition of different concentrations of glucose after treated by Triton-100. The arrows indicated the concentration of glucose: 0, 10,100, 500, 1000, 2000 μM.

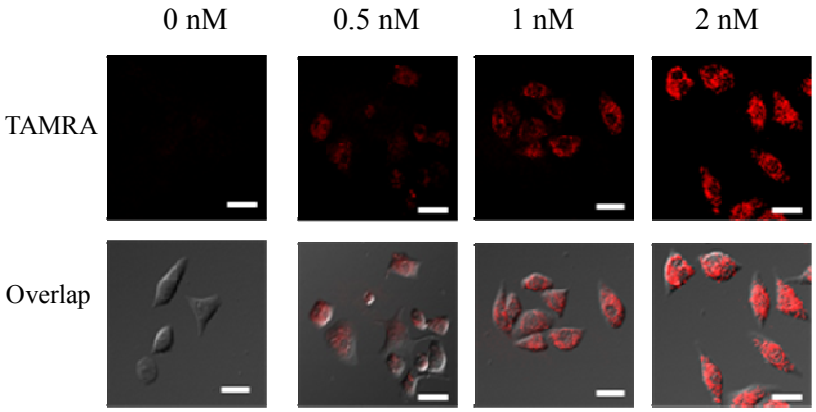

Figure S13. Confocal microscopy images recorded at TAMRA channel of the nanokit-treated HeLa cells as a function of different concentrations of nanokit.

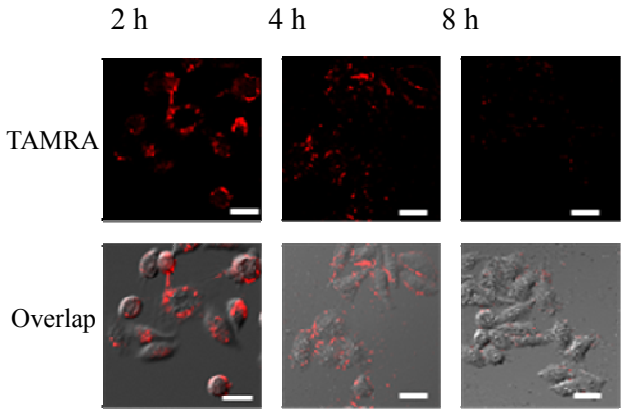

Figure S14. Intracellular glucose imaging of HeLa cells under 10% O_2 as functions of time. The concentration of the nanokit was 2 nM.